

# Synthesis, characterization, and biological studies of novel Ni(II) and Zn(II) complexes with 5-chloro-2-(phenylazo)pyridine

Luksamee Vittaya<sup>a,\*</sup>, Nararak Leesakul<sup>b</sup>, Saowanit Saithong<sup>b</sup>, Souwalak Phongpaichit<sup>c</sup>, Phoom Chumponanomakun<sup>d</sup>, Theerapoom Boonprab<sup>b</sup>, Kittipong Chainok<sup>d</sup>, Yuthana Tantirungrotechai<sup>d</sup>

<sup>a</sup> Faculty of Science and Fisheries Technology, Rajamangala University of Technology Srivijaya, Sikao, Trang 92150 Thailand

<sup>b</sup> Department of Chemistry and Centre for Innovation in Chemistry, Faculty of Science, Prince of Songkla University, Hat Yai, Songkhla 90110 Thailand

<sup>c</sup> Natural Products Research Centre and Department of Microbiology, Faculty of Science, Prince of Songkla University, Hat Yai, Songkhla 90110 Thailand

<sup>d</sup> Department of Physics, Faculty of Science and Technology, Thammasat University, Klong Luang, Pathumthani 12120 Thailand

\*Corresponding author, e-mail: nokluksamee@hotmail.com

Received 18 Sep 2015

Accepted 2 May 2017

**ABSTRACT:** An azoimine compound, 5-chloro-2-(phenylazo)pyridine (Clazpy), reacted with Ni(II) and Zn(II) sulphate salts and formed divalent metal complexes with a general formula of  $[M(\text{Clazpy})_2(\text{NCS})_2]$ , where M is Ni(II) or Zn(II). The synthesized complexes were characterized on the basis of elemental analysis, nuclear magnetic resonance, and infrared and electronic absorption spectroscopy. The single crystal X-ray diffraction and infrared data of the Zn(II) complex show that the ligand coordinates through the donating nitrogen atoms of the pyridine ring and azo moiety of Clazpy and N atoms of the thiocyanate groups. Our density functional theory calculations used the B3LYP/6-31G(d,p)&LANL2DZ functional and basis sets to predict the most favourable structures of  $[\text{Ni}(\text{Clazpy})_2(\text{NCS})_2]$  and  $[\text{Zn}(\text{Clazpy})_2(\text{NCS})_2]$ . The TD-CAM-B3LYP/6-31+G(d,p)&LANL2DZ electronic transition energies agree with the electronic spectra and hence confirm their structures. Minimal inhibitory concentrations (MIC) and minimal bactericidal concentrations or minimal fungicidal concentrations (MFC) of all tested compounds were determined against human pathogens by a colorimetric microdilution method. The Clazpy compound and its complexes are significantly active against yeast and filamentous fungus with MIC and MFC values of 32 and 200  $\mu\text{g}/\text{ml}$ , respectively. The Clazpy ligand showed higher antimicrobial activities against pathogenic yeast *Cryptococcus neoformans* (MIC/MFC 32/32  $\mu\text{g}/\text{ml}$ ) than both complexes (MIC/MFC 64/128  $\mu\text{g}/\text{ml}$ ). The  $[\text{Ni}(\text{Clazpy})_2(\text{NCS})_2]$  complex exhibited higher antimicrobial activities against fungal strains of *Microsporium gypseum* (MIC/MFC 64/128  $\mu\text{g}/\text{ml}$ ) than the  $[\text{Zn}(\text{Clazpy})_2(\text{NCS})_2]$  complex. These new azoimine metal complexes might therefore be considered as prospective antifungal agents.

**KEYWORDS:** azoimine compound, divalent metal complexes, DFT, antimicrobial activity, X-ray diffraction

## INTRODUCTION

Transition metal complexes with the azoimine ligand ( $-\text{N}=\text{N}-\text{C}=\text{N}-$ ) have been widely investigated for a long time because the  $\pi$ -acidity of this ligand helps stabilize low oxidation states of metal ions<sup>1-3</sup>. The applications of azoimine complexes are many and varied in industrial and pharmaceutical fields<sup>4,5</sup>. The versatility of  $[\text{Ru}(\text{azpy})_2\text{Cl}_2]$ , a well-known complex of ruthenium(II) with 2-(phenylazo)pyridine (azpy), has been extensively explored.

It is an effective catalyst in the epoxidation reaction of olefin<sup>6</sup> as well as an anticancer agent in various cancer cell lines<sup>5-7</sup>. Recently, other azpy derivatives and their ruthenium complexes have been synthesized: for example,  $[\text{Ru}(\text{Hszapy})_2\text{Cl}_2]$  when Hszapy = 2-phenylazo pyridine-5-sulphonic acid<sup>8</sup>,  $[\text{Ru}(\text{4mazpy})_2\text{Cl}_2]$  when 4mazpy = 4-methyl-2-phenylazopyridine<sup>5</sup>, and  $[\text{Ru}(\text{Clazpy})_2\text{Cl}_2]$  when Clazpy is 5-chloro-2-(phenylazo) pyridine<sup>9</sup>. The Clazpy compound is a derivative of the azpy compound with a chlorine atom at the meta-position

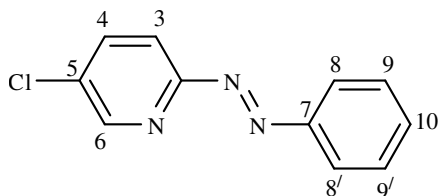


Fig. 1 Structure and  $^1\text{H}$ -numbering of Clazpy.

of the pyridine ring (Fig. 1). The ruthenium complexes of  $[\text{Ru}(\text{Clazpy})_2(\text{L})]\text{Cl}_2 \cdot x\text{H}_2\text{O}$ , where L is either 2,2'-bipyridine (bpy) or 1,10-phenanthroline (phen), have been studied for their DNA-binding properties<sup>10</sup>. However, coordination complexes of Clazpy with other metal ions are few<sup>11</sup>, and to our knowledge, their antimicrobial activities have not yet been reported. Hence we were interested in synthesizing novel complexes of Ni(II) and Zn(II) with Clazpy to yield the  $[\text{Ni}(\text{Clazpy})_2(\text{NCS})_2]$  and  $[\text{Zn}(\text{Clazpy})_2(\text{NCS})_2]$  complexes. We discuss the synthesis and spectroscopic characterization of both complexes and compare the findings with those reported for the  $[\text{Fe}(\text{Clazpy})_2(\text{NCS})_2]$  complex<sup>12</sup>. Electronic structure calculations using density functional theory (DFT) were carried out to deduce the most favourable structure of both complexes. Finally, we carried out a study on the antimicrobial activity of the Clazpy ligand and its complexes to explore their possibilities as antibacterial or antifungal agents.

## MATERIALS AND METHODS

### Materials

Ammonium thiocyanate ( $\text{NH}_4\text{NCS}$ ),  $\text{NiSO}_4$ , and  $\text{ZnSO}_4$  were purchased from Aldrich. The Clazpy (5-chloro-2-(phenylazo)pyridine) was prepared according to a previously reported procedure<sup>11</sup>. The synthesis of  $[\text{Ni}(\text{Clazpy})_2(\text{NCS})_2]$  and  $[\text{Zn}(\text{Clazpy})_2(\text{NCS})_2]$  was carried out similarly to that of the  $[\text{Fe}(\text{Clazpy})_2(\text{NCS})_2]$  complex reported elsewhere<sup>12</sup>. All solvents were of analytical reagent grade and were used without further purification.

### Synthesis of $[\text{Ni}(\text{Clazpy})_2(\text{NCS})_2]$ complex

The synthesis of this complex was adapted from that of  $[\text{Fe}(\text{Clazpy})_2(\text{NCS})_2]$  by Vittaya et al<sup>12</sup>. A stirred methanolic solution (10 ml) of ammonium thiocyanate (0.53 mmol, 0.04 g) was added dropwise to a methanolic solution of  $\text{NiSO}_4 \cdot 5\text{H}_2\text{O}$  (0.25 mmol, 0.07 g) at room temperature. After stirring continuously for 30 min, a white solid precipitated which was then filtered off and the filtrate was added to a

methanolic solution of Clazpy (0.50 mmol, 0.11 g). Later on, the reaction mixture was refluxed for 4 h and left standing overnight. A dark green solid was obtained.

### Synthesis of $[\text{Zn}(\text{Clazpy})_2(\text{NCS})_2]$ complex

The synthesis of this complex followed that of  $[\text{Ni}(\text{Clazpy})_2(\text{NCS})_2]$  but replacing  $\text{NiSO}_4 \cdot 5\text{H}_2\text{O}$  with  $\text{ZnSO}_4 \cdot 5\text{H}_2\text{O}$  (0.25 mmol, 0.07 g). After the reaction was refluxed, the orange solution was filtered and left standing for a few days. An orange solid was obtained.

### Physicochemical measurements

The carbon, hydrogen, nitrogen, and sulphur elemental analyses were measured with a CHNS/O analyser, CE Instruments Flash EA 1112 Series, Thermo Quest. FT-IR spectra were recorded on KBr pellets with a Bruker EQUINOX 55 Fourier transform infrared spectrometer in the range of 4000–400  $\text{cm}^{-1}$ . Electronic spectra were measured at room temperature on a U-1800 spectrophotometer equipped with quartz cuvettes of 1 cm path length. The  $^1\text{H}$  and  $^{13}\text{C}$  NMR spectra of complexes in chloroform- $d_3$  were obtained on a 500 MHz Varian UNITY INOVA Fourier transform NMR spectrometer. Melting points of all compounds were measured on an electrothermal melting point apparatus.

### X-ray determination

The complex of  $[\text{Zn}(\text{Clazpy})_2(\text{NCS})_2]$  was crystallized in a methanol solution. The X-ray diffraction data were collected using a Bruker APEX-II CCD diffractometer with graphite-monochromated Mo  $\text{K}\alpha$  radiation ( $\lambda = 0.71073 \text{ \AA}$ ), 33 925 reflections. The diffraction data were processed by SMART, SAINT v8.34A, and SADABS<sup>13</sup>. The structure was solved by SHELXS<sup>14</sup>. The anisotropic thermal parameters were refined to all non-hydrogen atoms. All hydrogen atoms were placed in calculated, ideal positions and refined as a riding model. One of the thiocyanate ligands had a strong thermal motion due to its disordered position and it was separated into two sets of positions (A and B) and treated during refinement. The OLEX2<sup>15</sup>, WINGXv2014.1<sup>16</sup>, and MERCURY3.5.1<sup>17</sup> programs were used to prepare the materials and molecular graphics for publication. The crystallographic data of  $[\text{Zn}(\text{Clazpy})_2(\text{NCS})_2]$  have been deposited at Cambridge Crystallographic Data Centre via [www.ccdc.cam.ac.uk/data\\_request/cif](http://www.ccdc.cam.ac.uk/data_request/cif) (or from the Cambridge Crystallographic Data Centre, 12 Union Road, Cambridge CB21EZ, UK; fax: +44 1223 336 033 or email

deposit@ccdc.cam.ac.uk) with the CCDC 1063404 and can be received upon request. The X-ray data are reported as supplementary crystallographic data.

### Computational studies

For each complex, several possible isomers were initially constructed. All complexes were then geometry optimized in the gas phase at the singlet ground state without symmetry constraints. We employed the Density Functional Theory (DFT) method using the B3LYP hybrid functional<sup>18,19</sup> with the LANL2DZ effective core potential basis set for the metal atoms and the 6-31G(d,p) basis set for the other atoms (H, C, N, S, and Cl)<sup>20,21</sup>. We confirmed optimized structures to be at energy minima by frequency calculations. For each complex, the lowest energy structure was considered to be the most favourable structure. Using this structure, the electronic excitation energy was predicted by the TD-CAM-B3LYP/6-31+G(d,p)&LANL2DZ computational method with the CPCM solvation model representing dichloromethane media. All theoretical calculations were carried out using GAUSSIAN 09<sup>22</sup>. AVOGADRO was used to visualize the molecular orbital involved in the spectroscopic transition<sup>23</sup>; and GAUSSSUM facilitated the analysis of the electronic transitions<sup>24</sup>.

### Antibacterial assay

The assay followed a microdilution method which is a modification of CLSI M07-A9 protocol<sup>25</sup>. All compounds were dissolved in dimethyl sulphoxide and were tested against *Staphylococcus aureus* ATCC25923, a clinical isolate of methicillin-resistant *S. aureus* (MRSA) SK1, *Escherichia coli* ATCC25922, and *Pseudomonas aeruginosa* ATCC27853. The minimal inhibitory concentrations (MICs) were the lowest concentration of the synthesized compounds that inhibited visible growth. Samples of the synthesized compounds that were less dilute than the

MIC and at the MIC were streaked onto a nutrient agar plate and incubated under appropriate conditions. The lowest concentration of compounds which showed no growth was recorded as the minimal bactericidal concentrations (MBC). The standard antibacterial agents Vancomycin (VM) and gentamicin (GM) were used as positive inhibitory controls.

### Antifungal assay

The MICs of the synthesized compounds were determined against yeasts (*Candida albicans* ATCC90028, *Cryptococcus neoformans* ATCC90112) by a modification of the microbroth dilution CLSI M27-A3 protocol<sup>26</sup> and against a clinical isolate of *Microsporum gypseum* MU-SH4 by a modification of the microbroth dilution CLSI M38-A2 protocol<sup>27</sup>. Microtitre plates were incubated at 35 °C for 24 h for *C. albicans*, 48 h at room temperature for *C. neoformans*, and 7 days at room temperature for *M. gypseum*. The minimal fungicidal concentrations (MFCs) of active compounds were determined by the streaking method on Sabouraud's dextrose agar. Amphotericin B (AMB) was used as a positive inhibitory control for yeasts and miconazole (MCZ) for *M. gypseum*.

## RESULTS AND DISCUSSION

### Synthesis and physical properties

The Clazpy compound is an unsymmetrical bidentate ligand (Fig. 1) which binds to a metal centre via the nitrogen atoms of pyridine ( $N_p$ ) and the azo ( $N_a$ ) moiety. From a methanolic solution of Ni(II) or Zn(II) sulphate and Clazpy in 1:2 molar ratio with the presence of ammonium thiocyanate, we obtained dark green and orange precipitates of  $[Ni(Clazpy)_2(NCS)_2]$  and  $[Zn(Clazpy)_2(NCS)_2]$ , respectively. The analytical and physical data for these novel complexes are listed in Table 1. The

**Table 1** The analytical and physical data for  $[Fe(Clazpy)_2(NCS)_2]$ ,  $[Ni(Clazpy)_2(NCS)_2]$ , and  $[Zn(Clazpy)_2(NCS)_2]$ .

| Complex<br>(empirical formula)                        | Mw<br>(g/mol)       | Colour     | m.p.<br>(°C)         | Yield<br>(%) | % Found (calculated)          |                             |                               |                               |
|---|---------------------|------------|----------------------|--------------|-------------------------------|-----------------------------|-------------------------------|-------------------------------|
|   |                     |            |                      |              | C                             | H                           | N                             | S                             |
| $FeC_{24}H_{16}N_8S_2Cl_2$<br>$[Fe(Clazpy)_2(NCS)_2]$ | 607.34 <sup>a</sup> | Green      | 230.1–230.5          | 80           | 47.07 <sup>a</sup><br>(47.47) | 2.56 <sup>a</sup><br>(2.66) | 17.98 <sup>a</sup><br>(18.45) | 10.39 <sup>a</sup><br>(10.56) |
| $NiC_{24}H_{16}N_8S_2Cl_2$<br>$[Ni(Clazpy)_2(NCS)_2]$ | 610.16              | Dark green | > 300<br>(decompose) | 80           | 46.52<br>(47.24)              | 2.71<br>(2.64)              | 18.45<br>(18.36)              | 9.35<br>(10.51)               |
| $ZnC_{24}H_{16}N_8S_2Cl_2$<br>$[Zn(Clazpy)_2(NCS)_2]$ | 616.84              | Orange     | 179.5–180.5          | 60           | 46.92<br>(46.73)              | 2.58<br>(2.61)              | 18.71<br>(18.17)              | 9.44<br>(10.39)               |

<sup>a</sup> reported in Ref. 12.

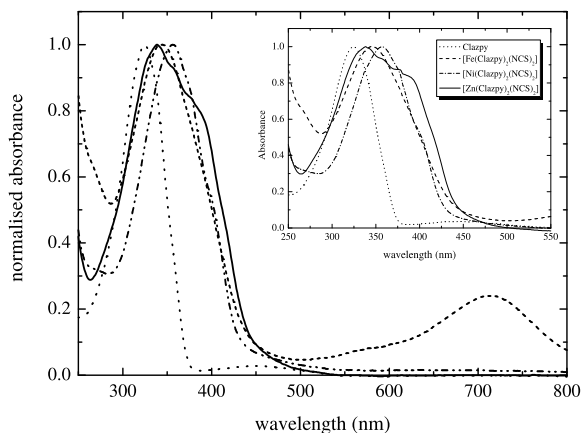


**Fig. 2** Electronic absorption spectra of Clazpy and the complexes  $[\text{Fe}(\text{Clazpy})_2(\text{NCS})_2]$ ,  $[\text{Ni}(\text{Clazpy})_2(\text{NCS})_2]$ , and  $[\text{Zn}(\text{Clazpy})_2(\text{NCS})_2]$  in dichloromethane solution.

elemental analysis indicates that the structural formulae of the synthesized Ni(II) and Zn(II) complexes are  $\text{NiC}_{24}\text{H}_{16}\text{N}_8\text{S}_2\text{Cl}_2$  and  $\text{ZnC}_{24}\text{H}_{16}\text{N}_8\text{S}_2\text{Cl}_2$ , respectively. The complex structures were elucidated using IR, UV-Vis and NMR spectroscopy.

#### UV-Vis studies

The UV-Vis spectra of the Clazpy compound and all complexes were recorded with  $1 \times 10^{-5}$  M in dichloromethane solutions (Fig. 2). We compared them with the free ligand spectra<sup>13</sup> and the spectral data of  $[\text{Fe}(\text{Clazpy})_2(\text{NCS})_2]$  for completion<sup>28</sup>. The electronic spectra of the studied complexes have similar features, especially between Fe(II) and Zn(II). The UV-Vis spectra of the  $[\text{Fe}(\text{Clazpy})_2(\text{NCS})_2]$  and  $[\text{Zn}(\text{Clazpy})_2(\text{NCS})_2]$  complexes exhibit two absorption bands. For  $[\text{Fe}(\text{Clazpy})_2(\text{NCS})_2]$ , they are at 346 nm ( $\epsilon \approx 3 \times 10^4 \text{ M}^{-1}\text{cm}^{-1}$ ) and at 714 nm ( $\epsilon \approx 10^4 \text{ M}^{-1}\text{cm}^{-1}$ ). The former band is assigned to an intraligand ( $\pi - \pi^*$ ) transition. The latter band is in the visible region assigned to a metal-to-ligand charge transfer (MLCT) transition for  $[\text{Fe}(\text{Clazpy})_2(\text{NCS})_2]$ <sup>28</sup>. This result was similarly observed in the  $[\text{Zn}(\text{Clazpy})_2(\text{NCS})_2]$  complex, which showed intense transition at 338 nm along with a weak transition around 450–460 nm. We assume that the first band may be assigned to an intraligand transition and that the latter refers to charge transfer between Zn(II) and the ligand<sup>29</sup>. This assignment for each complex is supported by oscillator strength, major assignments and character from TD-CAM-B3LYP calculations in dichloromethane solvent (Fig. 3). Since Clazpy is an effective  $\pi$ -acceptor ligand, coordination with

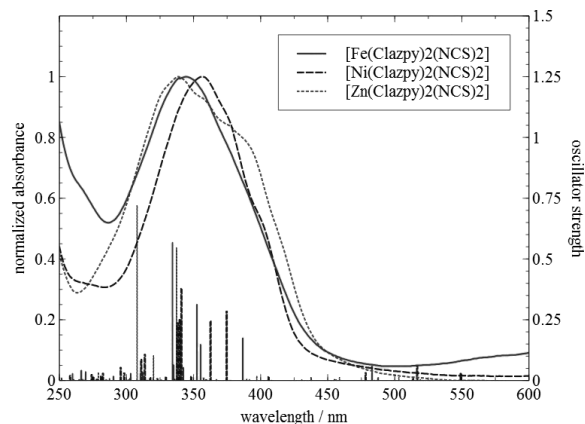


**Fig. 3** Electronic absorption spectra of the complexes  $[\text{Fe}(\text{Clazpy})_2(\text{NCS})_2]$ ,  $[\text{Ni}(\text{Clazpy})_2(\text{NCS})_2]$ , and  $[\text{Zn}(\text{Clazpy})_2(\text{NCS})_2]$  in dichloromethane solution. The TD/CAM-B3LYP/6-31+G(d,p)&LANL2DZ excitation energy and corresponding oscillator strength are shown as vertical lines.

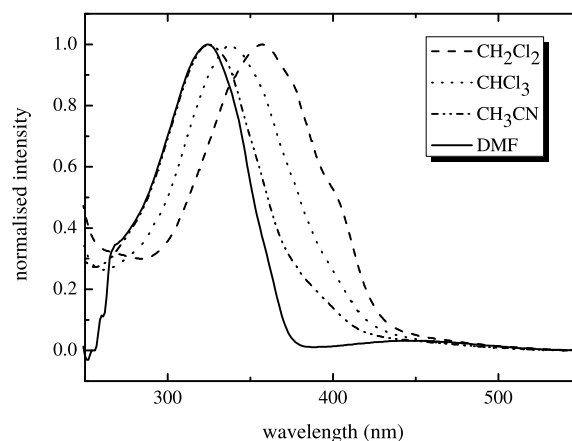


**Fig. 4** Electronic absorption spectra of the complex  $[\text{Ni}(\text{Clazpy})_2(\text{NCS})_2]$  in dichloromethane ( $\text{CH}_2\text{Cl}_2$ ), chloroform ( $\text{CHCl}_3$ ), acetonitrile ( $\text{CH}_3\text{CN}$ ), and dimethylformamide (DMF) solutions.

all electron rich metals like Fe(II) clearly yields the MLCT bands ( $\epsilon > 10^4 \text{ M}^{-1}\text{cm}^{-1}$ ). However, the  $[\text{Ni}(\text{Clazpy})_2(\text{NCS})_2]$  complex shows absorption at 357 nm ( $\epsilon \approx 3 \times 10^4 \text{ M}^{-1}\text{cm}^{-1}$ ). In addition, the  $\pi - \pi^*$  absorption band in the UV region of all the studied complexes is blue shifting with an increasing solvent polarity (Fig. 4). On the other hand, the MLCT band is only slightly changed with no apparent tendency. This indicates that the  $\pi$  orbital is stabilized by a high polarity solvent.

**Table 2** IR absorption ( $\text{cm}^{-1}$ ) band for the free ligand and its complexes.

| Compounds                                     | IR spectra ( $\text{cm}^{-1}$ ) <sup>†</sup> |                          |                          |                   |                  |                          |
|---|--|--------------------------|--------------------------|-------------------|------------------|--------------------------|
|   | $\nu(\text{C}=\text{C})$                     | $\nu(\text{N}=\text{C})$ | $\nu(\text{N}=\text{N})$ | $\nu(\text{NCS})$ | $\nu(\text{CS})$ | $\nu(\text{M}-\text{N})$ |
| Clazpy  | 1565(m)                                      | 1441(s)                  | 1364(s)                  | –                 | –                | –                        |
| [Fe(Clazpy) <sub>2</sub> (NCS) <sub>2</sub> ] | 1546(m),1588(m)                              | 1443(m),1457(m)          | 1344(s)                  | 2092(vs)          | 846(m)           | 460(w),474(w)            |
| [Ni(Clazpy) <sub>2</sub> (NCS) <sub>2</sub> ] | 1558(m),1588(m)                              | 1420(m),1452(m)          | 1379(s)                  | 2082(vs)          | 851(m)           | 438(w),476(w)            |
| [Zn(Clazpy) <sub>2</sub> (NCS) <sub>2</sub> ] | 1583(m),1558(m)                              | 1427(m),1440(m)          | 1373(s)                  | 2074(vs)          | 855(m)           | 434(w),476(w)            |

<sup>†</sup> vs = very strong; s = strong; m = medium; w = weak.

### Infrared (IR) studies

The infrared spectra of the free ligand and the complexes displayed many characteristic frequencies in the range of 4000–400  $\text{cm}^{-1}$  assigned to be the C=C, C=N, C–N(NCS), C–S(NCS), M–N, and, in particular, the N=N stretching frequencies which are reported in Table 2. The last band is consistent with N=N bonded to metal ion. Its frequency can be used as an indicator for the  $\pi$ -acceptor character between Clazpy ligands and its complexes. The N=N stretching frequencies in the complexes are around 1344–1379  $\text{cm}^{-1}$  while this mode appears at 1364  $\text{cm}^{-1}$  in the free Clazpy ligand<sup>11</sup>. This evidence confirmed the coordination of the Clazpy ligand to the metal centres as well as the function of the azo group to stabilize the lower oxidation state of the metal centres<sup>11</sup>. In addition, the strong sharp band around 2074–2092  $\text{cm}^{-1}$  corresponds to the  $\nu(\text{NCS})$  thiocyanate stretching frequency<sup>29–32</sup>. In this case, it has been indicated that the  $\nu_{\text{as}}(\text{C}\equiv\text{N})$  frequencies could be used as a criterion to differentiate between S-bonded (2110–2140  $\text{cm}^{-1}$ ) and N-bonded (< 2110  $\text{cm}^{-1}$ ) complexes<sup>33,34</sup>. Based on the stretching frequency, this analysis indicates that the binding mode of thiocyanate is N-bonded; this is similar to what has been observed in the literature<sup>33–35</sup>. Further confirmation resides in the absorption band at 846–855  $\text{cm}^{-1}$ , which is attributed to the  $\nu(\text{CS})$  stretching frequency of N-bonded ligands<sup>31,32</sup>; and in the weak intensity band around 434–476  $\text{cm}^{-1}$ , interpreted as the M–N stretching frequency.

### Nuclear magnetic resonance (NMR) studies

All complex structures were determined by using 1D and 2D NMR spectroscopic techniques (NMR, <sup>1</sup>H–<sup>1</sup>H COSY NMR, DEPT NMR, and HMQC NMR) in CDCl<sub>3</sub> except for [Ni(Clazpy)<sub>2</sub>(NCS)<sub>2</sub>] because of its solubility. The <sup>1</sup>H NMR spectrum of [Fe(Clazpy)<sub>2</sub>(NCS)<sub>2</sub>]<sup>28</sup> and [Zn(Clazpy)<sub>2</sub>(NCS)<sub>2</sub>] were assigned on the certain evidence of spin-spin interaction as

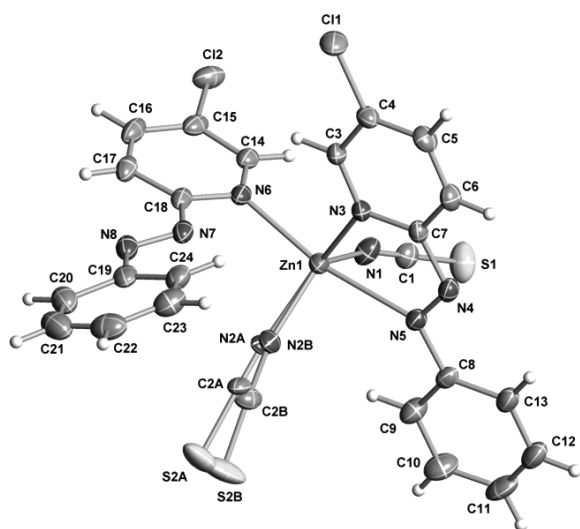
well as the chemical shifts and signal intensity. The coupling signals from pyridine protons occur at lower field than those of the phenyl protons. The signals obtained from the H6 proton in the pyridine rings appear at the lowest chemical shifts (8.96 ppm in [Fe(Clazpy)<sub>2</sub>(NCS)<sub>2</sub>], 8.68 ppm in [Ni(Clazpy)<sub>2</sub>(NCS)<sub>2</sub>], and 8.72 ppm in [Zn(Clazpy)<sub>2</sub>(NCS)<sub>2</sub>]) due to the influence of the coordinated nitrogen atom and the inductive effect of the chlorine atom. Furthermore, the signals from H3 and H4 protons occur at lower field than that of H8, H9, and H10 in the [Fe(Clazpy)<sub>2</sub>(NCS)<sub>2</sub>] complex, but they appear at higher field than that of H8 in [Ni(Clazpy)<sub>2</sub>(NCS)<sub>2</sub>] and [Zn(Clazpy)<sub>2</sub>(NCS)<sub>2</sub>]. The structure interpretation is also confirmed by the <sup>1</sup>H–<sup>1</sup>H COSY NMR spectroscopy. The <sup>13</sup>C NMR results corresponded to the DEPT (90) NMR which shows only methane carbon. The downfield signals are assigned to two quaternary carbons, C2 and C7, respectively. The high field signal is assigned to C5. However, the <sup>13</sup>C NMR signal assignments were based on <sup>1</sup>H–<sup>13</sup>C HMQC NMR spectra. Hence the results of 1D and 2D NMR spectra are helpful for assigning all signals. We conclude that all the synthesized complexes correspond to the expected complex structures.

### X-ray structure determination

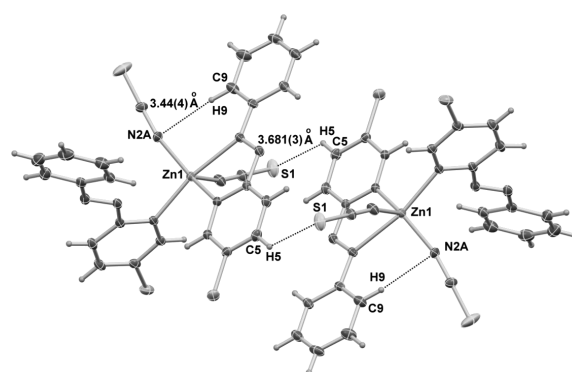
The complex of [Zn(Clazpy)<sub>2</sub>(NCS)<sub>2</sub>] was crystallized in methanol solution. The crystal data are summarized in Table 3. The X-ray structure adopts the five coordination of Zn(II) ion with two Clazpy ligands which is not commonly observed. The Zn(II) ion is coordinated by one chelating Clazpy, one monodentate via N(pyridine) atom and two thiocyanate ions through the N donor atom, generating the square pyramidal geometry (Fig. 5). The Zn–N(pyridine) distances of Zn1–N3 and Zn1–N6 are 2.066(2) and 2.185(2) Å, while the Zn–N(azo) distance of Zn1–N5 is 2.396(2) Å. The averaged Zn–N(pyridine) length of the synthesized compound is in agreement with some related square pyra-

**Table 3** Crystal data and structure refinement of  $[\text{Zn}(\text{Clazpy})_2(\text{NCS})_2]$ .

|                        |  |   |   |
|------------------------|--|---|---|
| Empirical formula      | $\text{C}_{24}\text{H}_{16}\text{Cl}_2\text{N}_8\text{S}_2\text{Zn}$   | $\theta$ range for data collection      | 2.911–25.395°   |
| Formula weight         | 616.84   | Index ranges                            | $-10 \leq h \leq 10, -34 \leq k \leq 34,$<br>$-12 \leq l \leq 12$ |
| Temperature            | 273(2) °K  | Reflections collected                   | 33 925  |
| Wavelength             | 0.71073 Å  | Independent reflections                 | 4926 [ $R(\text{int}) = 0.0322$ ]                                 |
| Crystal system         | Monoclinic   | Completeness to $\theta = 25.242^\circ$ | 99.8%   |
| Space group            | $P 2_1/c$  | Absorption correction                   | Semi-empirical from equivalents                                   |
| Unit cell dimensions   | $a = 9.1257(5)$ Å $\alpha = 90^\circ$<br>$b = 28.7986(16)$ Å $\beta = 91.711(2)^\circ$<br>$c = 10.2234(6)$ Å $\gamma = 90^\circ$ | Max. and min. transmission              | 0.7452 and 0.6330   |
| Volume                 | $2685.6(3)$ Å <sup>3</sup>   | Refinement method                       | Full-matrix least-squares on $F^2$                                |
| $Z$                    | 4  | Data / restraints / parameters          | 4926 / 66 / 362   |
| Density (calculated)   | 1.526 Mg/m <sup>3</sup>  | Goodness-of-fit on $F^2$                | 1.098   |
| Absorption coefficient | 1.299 mm <sup>-1</sup>   | Final $R$ indices [ $I > 2(I)$ ]        | $R1 = 0.0355, wR2 = 0.0744$                                       |
| $F(000)$               | 1248   | $R$ indices (all data)                  | $R1 = 0.0447, wR2 = 0.0779$                                       |
| Crystal size           | $0.300 \times 0.280 \times 0.280$ mm <sup>3</sup>  | Extinction coefficient                  | n/a   |
|                        |  | Largest diff. peak and hole             | 0.712 and $-0.547$ e/Å <sup>3</sup>                               |

**Fig. 5** X-ray structure of  $[\text{Zn}(\text{Clazpy})_2(\text{NCS})_2]$ .

midal compounds like  $[\text{Zn}(\text{Py})(\text{chxn})(\text{Cl}-\text{sal})_2]$ , for which the average length is  $2.116(3)$  Å<sup>36</sup>, and the  $[\text{Zn}(\text{BCIP})\text{Cl}_2]$  complex, for which it is  $2.063(1)$  Å<sup>37</sup>. The dihedral angle of the pyridine ring and the phenyl ring of the chelating Clazpy ligand is  $5.387^\circ$ . It is different from that obtained from the monodentate Clazpy ( $29.612^\circ$ ) which is in *trans* between the azopyridine and phenyl rings. The azo ( $\text{N}=\text{N}$ ) bond lengths between a chelating Clazpy and a monodentate are the same at  $1.250(3)$  Å, which is longer than that of the free Clazpy ligand at  $1.234(2)$  Å<sup>38</sup>. This lengthening supports the majority of the  $\sigma$ -donor and  $\pi$ -acceptor character of the Clazpy ligand from  $d^{10}-\pi^*$  orbital of the azo moiety. The  $\text{Zn}-\text{N}(\text{SCN})$  distances of  $\text{Zn1}-\text{N1}$

**Fig. 6** Intra-hydrogen bonding between the phenyl ring of Clazpy and  $\text{N}(\text{SCN})$  in  $[\text{Zn}(\text{Clazpy})_2(\text{NCS})_2]$ .

and the averaged distance of  $\text{Zn1}-\text{N2A}$  or  $\text{Zn1}-\text{N2B}$  are similar which are  $1.974(2)$  Å and  $1.96(2)$  Å, respectively.

There is a  $\text{C9}-\text{H9}\cdots\text{N2A}$  intra-hydrogen bonding of  $3.44(4)$  Å between the phenyl ring of Clazpy and  $\text{N}(\text{SCN})$ . In addition, a pair of alternated weak inter-hydrogen bonds  $\text{C5}-\text{H5}\cdots\text{S1}\#_1$  ( $\#1 -x, -y + 1, -z + 1$ ) between the pyridine ring and  $\text{S}(\text{SCN})$  of adjacent molecules is observed, with the distance of  $3.681(3)$  Å (Fig. 6). In the crystal packing, the  $\text{C}-\text{Cl}-\pi$  interactions are detected between  $\text{Cl1}$  atom of the chelating Clazpy and the phenyl centroid ( $\text{Cg5}$ ) of the monodentate Clazpy. These interactions are also found between  $\text{Cl2}$  and the phenyl centroid ( $\text{Cg3}$ ) of two adjacent monodentate Clazpy ligands. Furthermore, all  $\text{Cl}-\pi$  contacts form a 3D interaction network as depicted in Fig. 7.

We note that the structural comparison with  $[\text{Ni}(\text{Clazpy})_2(\text{SCN})_2]$  is unsuccessful as its single

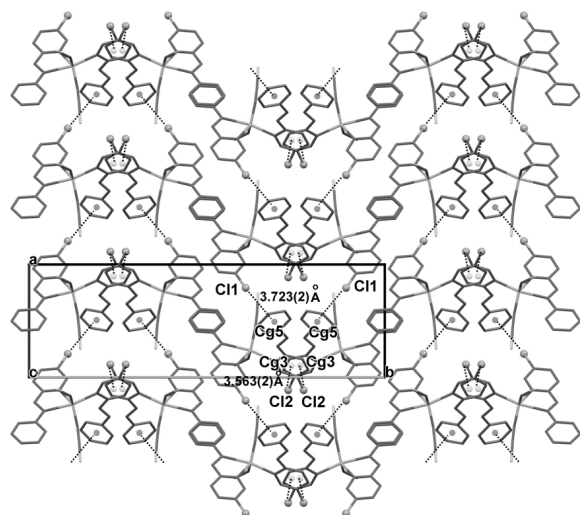


**Fig. 7** Intermolecular force of C–Cl– $\pi$  interactions in  $[\text{Zn}(\text{Clazpy})_2(\text{NCS})_2]$ .

crystal cannot be obtained. Hence we resorted to DFT calculation to deduce its structure. We tested the validity of the DFT calculations for  $[\text{Ni}(\text{Clazpy})_2(\text{SCN})_2]$  by calculating the structure of  $[\text{Fe}(\text{Clazpy})_2(\text{SCN})_2]$ , of which the X-ray structure is known. The B3LYP/6-31G(d,p)&LANL2DZ computational method reproduced the  $[\text{Fe}(\text{Clazpy})_2(\text{SCN})_2]$  structure well. Hence we believe that the calculated  $[\text{Ni}(\text{Clazpy})_2(\text{SCN})_2]$  structure is justified.

#### DFT/TDDFT calculations

Fig. 8 displays the B3LYP/6-31G(d,p) optimized structures of  $[\text{Fe}(\text{Clazpy})_2(\text{NCS})_2]$ ,  $[\text{Zn}(\text{Clazpy})_2(\text{NCS})_2]$ , and  $[\text{Ni}(\text{Clazpy})_2(\text{NCS})_2]$  complexes. The selected bond lengths and bond angles are summarized in Tables 4 and 5. As the X-ray structure of  $[\text{Fe}(\text{Clazpy})_2(\text{NCS})_2]$  is known, we used it to validate our calculations. For the  $[\text{Fe}(\text{Clazpy})_2(\text{NCS})_2]$  complex, which has distorted octahedral geometry, the calculated geometry parameters agree with the single-crystal X-ray results. The bond lengths differ not more than 0.04 Å. For the Zn(II) complex, a new compound with a known X-ray structure, the *trans-cis-cis* (tcc) configuration was the most stable form. The two Clazpy ligands interact differently with the Zinc(II) ion, as different Zn–N(azo) distances are observed. The longest Zn–N(azo) distances are 2.460 Å and the angle around the central metal ion diverges from the 90° angle of the ideal octahedral structure. Interestingly, an optimized structure of  $[\text{Ni}(\text{Clazpy})_2(\text{NCS})_2]$ , with an octahedral initial

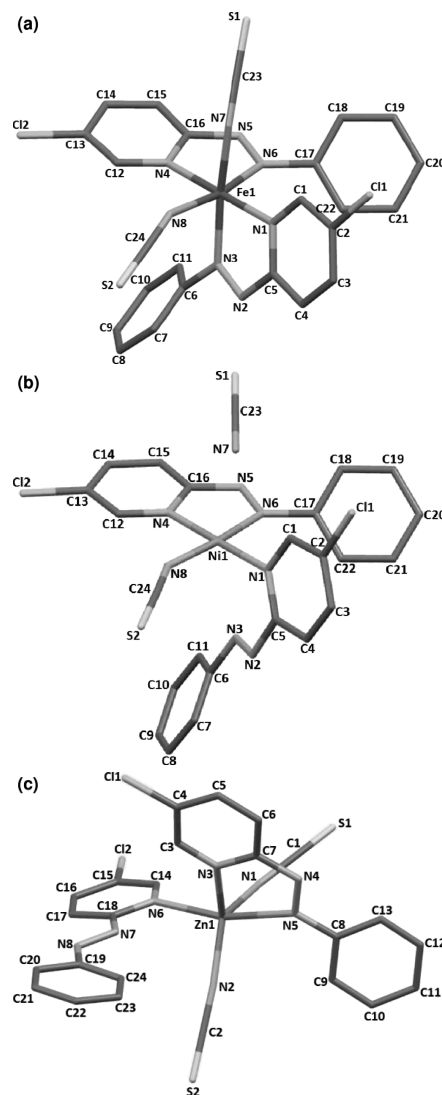


**Fig. 8** The optimized structures of (a)  $[\text{Fe}(\text{Clazpy})_2(\text{NCS})_2]$ , (b)  $[\text{Ni}(\text{Clazpy})_2(\text{NCS})_2]$ , and (c)  $[\text{Zn}(\text{Clazpy})_2(\text{NCS})_2]$ . Hydrogen atoms are omitted for clarity.

geometry, has two Clazpy and two thiocyanate ligands coordinated to the nickel ion in square planar fashion. The thiocyanate ligands bind with all complexes using the nitrogen atom as the donor atom. However, the Clazpy ligands bind with the nickel ion using two monodentate Ni $\cdots$ N(py) bonds. This differs from the Fe(II) and Zn(II) complexes, the structures of which are more or less octahedral. We observed large Ni–N3(azo) and Ni–N7(SCN) distances around 2.67 Å. These distances were distinctly longer than the other Ni–N bonds which are on average 1.936 Å. This is probably a manifestation of the Jahn-Teller distortion that lengthens Ni–N

**Table 4** Selected bond lengths (Å) and bond angles (°) for [Fe(Clazpy)<sub>2</sub>(NCS)<sub>2</sub>] and [Ni(Clazpy)<sub>2</sub>(NCS)<sub>2</sub>] at B3LYP/6-31G(d,p)&LANL2DZ calculation along with X-ray data.

| Optimized geometry | [Fe(Clazpy) <sub>2</sub> (NCS) <sub>2</sub> ] |                   | [Ni(Clazpy) <sub>2</sub> (NCS) <sub>2</sub> ] |
|--------------------|---|-------------------|---|
|                    | Calc.   | Exp. <sup>†</sup> | Calc.   |
| M1–N3              | 1.968   | 1.900             | 2.691   |
| M1–N6              | 1.968   | 1.917             | 1.969   |
| M1–N4              | 1.974   | 1.936             | 1.926   |
| M1–N7              | 1.976   | 1.941             | 2.641   |
| M1–N1              | 1.974   | 1.945             | 1.965   |
| M1–N8              | 1.975   | 1.952             | 1.884   |
| N1–C1              | 1.335   | 1.336             | 1.342   |
| N1–C5              | 1.353   | 1.352             | 1.356   |
| N2–N3              | 1.274   | 1.282             | 1.261   |
| N3–C6              | 1.427   | 1.433             | 1.412   |
| N7–C23             | 1.187   | 1.144             | 1.184   |
| N8–C24             | 1.187   | 1.156             | 1.193   |
| C2–C11             | 1.738   | 1.722             | 1.739   |
| N3–M1–N1           | 79.17   | 79.49             | 69.03   |
| N6–M1–N1           | 101.40  | 99.78             | 100.05  |
| N3–M1–N8           | 84.00   | 85.23             | 85.10   |
| N1–M1–N8           | 87.54   | 89.68             | 88.13   |
| C1–N1–M1           | 128.25  | 130.10            | 117.45  |
| C5–N1–M1           | 111.64  | 111.03            | 122.68  |
| N2–N3–M1           | 117.83  | 118.86            | 103.00  |
| C6–N3–M1           | 127.45  | 125.00            | 131.91  |

<sup>†</sup> reported in Ref. 12.

bonds along the *z*-direction. The square planar structure is observed in the [Ni(Clazpy)<sub>2</sub>(NCS)<sub>2</sub>] optimized structures regardless of the initial structures used in the geometry optimization.

The electronic absorption spectra of the complexes were characterized using the TD-CAM-B3LYP/6-31+G(d,p)&LANL2DZ method with the CPCM solvation model representing dichloromethane. There is general agreement between the experimental spectra and computational transitions. The [Fe(Clazpy)<sub>2</sub>(NCS)<sub>2</sub>] complex possesses an absorption band around 300–400 nm. This can be characterized as ligand-to-ligand transitions: LLCT within the Clazpy ligand and ILCT from Clazpy to SCN<sup>−</sup> ligands, at 352.5 nm (*f* = 0.313) and 334.3 nm (*f* = 0.567), respectively; and as metal-to-ligand charge transfer transition from iron ion to Clazpy ligands at 487.6 nm (*f* = 0.012) and 437.5 nm (*f* = 0.012). For the [Ni(Clazpy)<sub>2</sub>(NCS)<sub>2</sub>] complex, the calculated transition energies fall in the same region as an experimental band around 300–380 nm. The character of electronic transitions in this region is composed of ILCT within Clazpy and a small con-

**Table 5** Selected bond lengths (Å) and bond angles (°) for [Zn(Clazpy)<sub>2</sub>(NCS)<sub>2</sub>] at B3LYP/6-31G(d,p)&LANL2DZ calculation along with X-ray data.

| Optimized geometry | [Zn(Clazpy) <sub>2</sub> (NCS) <sub>2</sub> ] |        |
|--------------------|---|--------|
|                    | Calc.   | Exp.   |
| Zn1–N1             | 2.013   | 1.974  |
| Zn1–N2             | 1.986   | 2.020  |
| Zn1–N3             | 2.213   | 2.066  |
| Zn1–N5             | 2.425   | 2.396  |
| Zn1–N6             | 2.285   | 2.185  |
| N1–C1              | 1.192   | 1.146  |
| N2–C2              | 1.189   | 1.250  |
| N3–C3              | 1.336   | 1.335  |
| N3–C7              | 1.349   | 1.345  |
| N4–N5              | 1.264   | 1.250  |
| N5–C8              | 1.408   | 1.430  |
| N6–C14             | 1.339   | 1.335  |
| N6–C18             | 1.347   | 1.342  |
| N7–N8              | 1.262   | 1.250  |
| N8–C19             | 1.407   | 1.423  |
| C4–Cl1             | 1.741   | –      |
| N3–Zn1–N5          | 65.50   | 71.33  |
| N3–Zn1–N6          | 99.23   | 98.97  |
| N1–Zn1–N3          | 104.93  | 111.67 |
| N2–Zn1–N3          | 123.25  | 122.50 |
| N1–Zn1–N2          | 128.24  | 120.10 |
| N2–Zn1–N5          | 95.58   | 94.60  |
| N2–Zn1–N6          | 97.74   | 96.20  |

tribution from MLCT between the nickel ion and Clazpy at 374.7 and 362.6 nm. The transition at the shoulder is assigned to LLCT from Clazpy to SCN<sup>−</sup> ligands. Finally, for the [Zn(Clazpy)<sub>2</sub>(NCS)<sub>2</sub>] complex, an intense band is assigned to an intense ILCT at 307.9 nm (*f* = 0.721) and another ILCT at 337.3 nm (*f* = 0.546). Both are due to the  $\pi - \pi^*$  transition within Clazpy. For this series of complexes, the ILCT transition from within Clazpy is a dominant transition. The MLCT plays some role in the electronic transitions of [Fe(Clazpy)<sub>2</sub>(NCS)<sub>2</sub>] and [Ni(Clazpy)<sub>2</sub>(NCS)<sub>2</sub>] complexes but not in the [Zn(Clazpy)<sub>2</sub>(NCS)<sub>2</sub>] complex.

#### Antimicrobial activity of the compounds

Using an agar microdilution method, the antimicrobial activity of the new compounds was tested against four bacteria, namely, *S. aureus* (SA), methicillin-resistant *S. aureus* (MRSA), *P. aeruginosa* ATCC27853 (PA) and *E. coli* ATCC25922 (EC), yeasts (*C. albicans* ATCC 90028 and *C. neoformans* ATCC 90112) and fungus (*M. gypseum*). It is compared with the activity of standard antibacterial

**Table 6** Antibacterial activities of Clazpy and its Fe(II), Ni(II), and Zn(II) complexes.<sup>†</sup>

| Activity                             | MIC/MBC or MFC ( $\mu\text{g/ml}$ ) |        |        |           |       |       |             |       |
|--------------------------------------|-------------------------------------|--------|--------|-----------|-------|-------|-------------|-------|
|                                      | Clazpy                              | FCN    | NCN    | ZCN       | VM    | GM    | AMB         | MCZ   |
| Anti- <i>S. aureus</i> ATCC25923     | > 200                               | > 200  | > 200  | > 200     | 0.5/1 | –     | –           | –     |
| Anti-MRSA-SK1                        | > 200                               | > 200  | > 200  | > 200     | 0.5/1 | –     | –           | –     |
| Anti- <i>P. aeruginosa</i> ATCC27853 | > 200                               | > 200  | > 200  | > 200     | –     | 0.5/1 | –           | –     |
| Anti- <i>E. coli</i> ATCC25922       | > 200                               | > 200  | > 200  | > 200     | –     | 0.5/1 | –           | –     |
| Anti- <i>C. albicans</i> ATCC90028   | > 200                               | > 200  | > 200  | > 200     | –     | –     | 0.063/0.125 | –     |
| Anti- <i>C. neoformans</i> ATCC90112 | 32/32                               | 32/128 | 64/128 | 64/128    | –     | –     | 0.25/0.5    | –     |
| Anti- <i>M. gypseum</i> MU-SH4       | 32/128                              | 32/64  | 64/128 | 128/> 200 | –     | –     | –           | 0.5/8 |

<sup>†</sup> MRSA = methicillin resistant *S. aureus*, Clazpy = 5-Chloro-2-(phenylazo)pyridine, FCN =  $[\text{Fe}(\text{Clazpy})_2(\text{NCS})_2]$ , NCN =  $[\text{Ni}(\text{Clazpy})_2(\text{NCS})_2]$ , ZCN =  $[\text{Zn}(\text{Clazpy})_2(\text{NCS})_2]$ , VM = vancomycin, GM = gentamicin, AMB = amphotericin B, MCZ = miconazole.

drugs, vancomycin and gentamicin, and standard antifungal drugs, amphotericin B and miconazole, as presented in Table 6. Since DMSO was used as the solvent, it too was checked against each test organism but showed no activity.

From the in vitro antibacterial assay, it is observed that all tested compounds show no antibacterial activities at concentrations greater than 200  $\mu\text{g/ml}$ . However, Clazpy and its complexes significantly inhibited *C. neoformans* and *M. gypseum*. In particular, Clazpy exhibited the best antifungal activity against *C. neoformans* with MIC/MFC values of 32/32  $\mu\text{g/ml}$  and  $[\text{Fe}(\text{Clazpy})_2(\text{NCS})_2]$  gave the best inhibition of *M. gypseum* with MIC/MFC of 32/64  $\mu\text{g/ml}$ . The variations in the antimicrobial activities of the free ligand and the metal complexes against different microorganisms depend either on the impermeability of the microbe cells or on differences in the ribosomes in the microbial cells<sup>39</sup>. This would suggest that chelation could enhance the transport of complexes across the cell membrane of the microorganisms by reducing the polarizability of the metal complex, as postulated by Tweedy's chelation theory<sup>40</sup>.

## CONCLUSIONS

Two novel complexes were synthesized. The analytical data and the spectroscopic studies suggested that the complexes had the general formula  $[\text{M}(\text{Clazpy})_2(\text{NCS})_2]$  where M is Ni(II) and Zn(II). According to the UV-Vis and IR data, Clazpy was coordinated to the metal ion through the nitrogen atoms from pyridine and the azo moiety. The thiocyanate ligands bind to the metal ion through their nitrogen atom. These experimental data are in line with DFT calculations, as most of the possible conformations were distorted octahedral rather than

square planar. Furthermore, this study provides new insights to previously unpublished information on the antibacterial potential and effectiveness of new azoimine complexes of Fe(II), Ni(II) and Zn(II). The results of the in vitro antimicrobial assays of the ligand and its metal complexes clearly show that the Clazpy compound and its complexes have a significant antifungal activity against *C. neoformans* and *M. gypseum*. However, it shows no antibacterial activity even at high concentration (MIC > 200  $\mu\text{g/ml}$ ).

**Acknowledgements:** The author would like to thank the Faculty of Science and Fisheries Technology, Rajamangala University of Technology Srivijaya, Trang campus for financial support. We express our thanks for partial financial support and the single crystal X-ray diffractometer to the Centre for Innovation in Chemistry (PERCH-CIC), Commission on Higher Education, Ministry of Education. We would also like to thank Mr Thomas Duncan Coyne for assistance with the English.

## REFERENCES

1. Krause RA, Krause K (1980) Chemistry of bipyridyl-like ligands. Isomeric complexes of ruthenium(II) with 2-(phenylazo)pyridine. *Inorg Chem* **19**, 2600–3.
2. Seal A, Ray S (1984) Structures of two isomers of dichlorobis(2-phenylazopyridine) ruthenium(II),  $[\text{RuCl}_2(\text{C}_{11}\text{H}_9\text{N}_3)_2]$ . *Acta Crystallogr* **C40**, 929–32.
3. Velder AH, Schilden KVD, Hotze ACG, Reedijk J, Kooijman H, Spek AL (2004) Dichlorobis(2-phenylazopyridine)ruthenium(II) complexes: characterization, spectroscopic and structural properties of four isomers. *Dalton Trans* **3**, 448–55.
4. Barf GA, Sheldon RA (1995) Ruthenium(II) 2-(phenylazo)pyridine complexes as epoxidation catalysts. *J Mol Catal* **98**, 143–6.
5. Hotze ACG, Caspers SE, de Vos D, Kooijman H, Spek AL, Flamigni A, Bacao M, Sava G, Haasnoot

- JG, Reedijk J (2004) Structure-dependent in vitro cytotoxicity of the isomeric complexes  $[\text{Ru}(\text{L})_2\text{Cl}_2]$  ( $\text{L} = o\text{-tolylazopyridine}$  and  $4\text{-methyl-2-phenylazopyridine}$ ) in comparison to  $[\text{Ru}(\text{azpy})_2\text{Cl}_2]$ . *J Biol Inorg Chem* **9**, 354–64.
6. Hotze ACG, Bacac M, Velders AH, Jansen BAJ, Kooijman H, Spek AL, Haasnoot JG, Reedijk J (2003) New cytotoxic and water-soluble bis(2-phenylazopyridine) ruthenium(II) complexes. *J Med Chem* **46**, 1743–50.
  7. Velders AH, Kooijman H, Spek AL, Haasnoot JG, de Vos D, Reedijk J (2000) Strong differences in the in vitro cytotoxicity of three isomeric dichlorobis(2-phenylazopyridine)ruthenium(II) complexes. *Inorg Chem* **39**, 2966–7.
  8. Hotze ACG, Kooijman H, Spek AL, Haasnoot JG, Reedijk J (2004) Synthesis and characterization of ruthenium(II) complexes with the new ligand 2-phenylazopyridine-5-sulfonic acid (Hsazpy): in search for new anticancer agents. *New J Chem* **28**, 565–9.
  9. Hansongnern K, Sahavisit L, Pakawatchai C (2008) Crystal structure of *cis*-bis(5-chloro-2-(phenylazo)pyridine)dichlororuthenium(II). *Anal Sci* **24**, x57–8.
  10. Rattanaphan A, Nhukeaw T, Temboot P, Hansongnern K (2012) DNA-binding properties of ruthenium(II) complexes with the bidentate ligand 5-chloro-2-(phenylazo)pyridine. *Transit Met Chem* **37**, 207–14.
  11. Sahavisit L, Hansongnern K (2005) Synthesis, spectral studies and electro chemical properties of ruthenium(II) complex with the new bidentate ligand 5-chloro-2-(phenylazo)pyridine. *Songklanakarinn J Sci Tech* **27**, 751–9.
  12. Vittaya L, Leesakul N, Pakawatchai C, Saitong S, Hansongnern K (2012) Bis[5-chloro-2-(phenyldiazonyl- $\kappa\text{N}^2$ )pyridine- $\kappa\text{N}$ ]bis(thiocyanato- $\kappa\text{N}$ )iron(II). *Acta Crystallogr* **E68**, m555–6.
  13. Bruker (2013) *SMART*, *SAINT v8.34A*, and *SADABS*, Bruker AXS Inc, Madison, WI.
  14. Sheldrick GM (2008) A short history of SHELX. *Acta Crystallogr* **A64**, 112–22.
  15. Dolomanov OV, Bourhis LJ, Gildea RJ, Howard JAK, Puschmann H (2009) *OLEX2*: a complete structure solution, refinement and analysis program. *J Appl Crystallogr* **42**, 339–41.
  16. Farrugia LJ (2012) *WinGX* and *ORTEP for Windows*: an update. *J Appl Crystallogr* **45**, 849–54.
  17. Macrae CF, Bruno IJ, Chisholm JA, Edgington PR, McCabe P, Pidcock E, Rodriguez-Monge L, Taylor R, van de Streek J, Wood PA (2008) *Mercury CSD 2.0* – new features for the visualization and investigation of crystal structures. *J Appl Crystallogr* **41**, 466–70.
  18. Becke AD (1993) Density-functional thermochemistry. III. The role of exact exchange. *J Chem Phys* **98**, 5648–52.
  19. Stephens PJ, Devlin FJ, Chabalowski CF, Frisch MJ (1994) Ab initio calculation of vibrational absorption and circular dichroism spectra using density functional force fields. *J Phys Chem* **98**, 11623–7.
  20. Francl MM, Pietro WJ, Hehre WJ, Binkley JS, Gordon MS, DeFrees DJ, Pople JA (1982) Self-consistent molecular orbital methods. XXIII. A polarization-type basis set for second-row elements. *J Chem Phys* **77**, 3654–65.
  21. Hay PJ, Wadt WR (1985) *Ab initio* effective core potentials for molecular calculations. Potentials for the transition metal atoms Sc to Hg. *J Chem Phys* **82**, 270–83.
  22. Frisch MJ, Trucks GW, Schlegel HB, Scuseria GE, Robb MA, Cheeseman JR, Scalmani G, Barone V, et al (2009) *Gaussian 09, Revision A.01*, Gaussian, Inc, Wallingford, CT.
  23. Hanwell MD, Curtis DE, Lonie DC, Vandermeersch T, Zurek E, Hutchison GR (2012) Avogadro: an advanced semantic chemical editor, visualization, and analysis platform. *J Cheminform* **4**, 17.
  24. O'Boyle NM, Tenderholt AL, Langner KM (2008) cclib: A library for package-independent computational chemistry algorithms. *J Comput Chem* **29**, 839–45.
  25. Clinical and Laboratory Standards Institute (2012) *Methods for Dilution Antimicrobial Susceptibility Tests for Bacteria that Grow Aerobically*, approved standard, 9th edn, CLSI document M07–A9, CLSI, Wayne, PA.
  26. Clinical and Laboratory Standards Institute (2008) *Reference Method for Broth Dilution Antifungal Susceptibility Testing of Yeasts*, approved standard, 3rd edn, CLSI documents M27–A3, CLSI, Wayne, PA.
  27. Clinical and Laboratory Standards Institute (2008) *Reference Method for Broth Dilution Antifungal Susceptibility Testing of Filamentous Fungi*, approved standard, 2nd edn, CLSI documents M38–A2, CLSI, Wayne, PA.
  28. Vittaya L, Leesakul N, Hansongnern K (2012) NMR Study of  $[\text{Fe}(\text{Clazpy})_2(\text{NCS})_2]$ . In: *Proceedings of the 6th Pure and Applied Chemistry International Conference*, Chiang Mai, Thailand, pp 1764–7.
  29. Chand BG, Ray US, Cheng J, Lu TH, Sinha C (2003) Studies on the zinc(II)-azoimine system. Single-crystal X-ray structure of  $\text{Zn}(\text{MeaaiMe})\text{Cl}_2 \cdot \text{H}_2\text{O}$  and  $\text{Zn}(\text{HaaiMe})_2(\text{NCS})_2$  (MeaaiMe = 1-methyl-2-(*p*-tolylazo)imidazole, HaaiMe = 1-methyl-2-(phenylazo)imidazole). *Polyhedron* **22**, 1213–9.
  30. Ray U, Banerjee D, Chantrapromma S, Fun HK, Lin JN, Lu TH, Sinha C (2005) Cobalt(II)-azoimidazole complexes: structures of  $[\text{Co}(\text{MeaaiMe})_4](\text{ClO}_4)_2 \cdot \text{H}_2\text{O}$  and  $[\text{Co}(\text{HaaiMe})_2(\text{NCS})_2]$  (MeaaiMe = 1-methyl-2-(*p*-tolylazo)imidazole; HaaiMe = 1-methyl-2-(phenylazo)imidazole). *Polyhedron* **24**, 1071–8.
  31. Youngme S, Chaichit N, Pakawatchai C, Booncoon S (2002) The coordination chemistry of mono and bis(di-2-pyridylamine) copper(II) complexes:

- preparation, characterization and crystal structures of  $[\text{Cu}(\text{L})(\text{NO}_2)_2]$ ,  $[\text{Cu}(\text{L})(\text{H}_2\text{O})_2(\text{SO}_4)]$ ,  $[\text{Cu}(\text{L})_2(\text{NCS})(\text{SCN}) \cdot 0.5\text{DMSO}]$  and  $[\text{Cu}(\text{L})_2(\text{SCN})_2]$ . *Polyhedron* **21**, 1279–88.
32. Gup R, Giziroglu E, Kirkan B (2007) Synthesis and spectroscopic properties of new azo-dyes and azo-metal complexes derived from barbituric acid and aminoquinoline. *Dyes Pigments* **73**, 40–6.
  33. Mautner FA, Louka FR, LeGuet T, Massoud SS (2009) Pseudohalide copper(II) complexes derived from polypyridyl ligands: synthesis and characterization. *J Mol Struct* **919**, 196–203.
  34. Mukhopadhyay U, Bernal I, Massoud SS, Mautner FA (2004) Syntheses, structure and some electrochemistry of Cu(II) complexes with tris[(2-pyridyl)methyl]amine:  $[\text{Cu}\{\text{N}(\text{CH}_2\text{-py})_3\}(\text{N}_3)]\text{ClO}_4$  (I),  $[\text{Cu}\{\text{N}(\text{CH}_2\text{-py})_3\}(\text{O}-\text{NO})]\text{ClO}_4$  (II) and  $[\text{Cu}\{\text{N}(\text{CH}_2\text{-py})_3\}(\text{NCS})]\text{ClO}_4$  (III). *Inorg Chim Acta* **357**, 3673–82.
  35. Ray U, Banerjee D, Liou JC, Lin CN, Lu TH, Sinha C (2005) Iron(II) and nickel(II)-thiocyanato complexes of 1-alkyl-2-(aryloxy)imidazole: single crystal X-ray structure of  $[\text{Fe}(\text{MeaiEt})_2(\text{NCS})_2]$  (MeaiEt = 1-ethyl-2-(p-tolylazo)imidazole) and  $[\text{Ni}(\text{MeaiMe})(\text{NCS})_2(\text{H}_2\text{O})_2] \cdot 2\text{DMF}$  (MeaiMe = 1-methyl-2-(p-tolylazo)imidazole). *Inorg Chim Acta* **358**, 1019–26.
  36. Szlyk E, Wojtczak A, Surdykowski A, Goździkiewicz M (2005) Five-coordinate zinc(II) complexes with optically active Schiff bases derived from (1R,2R)-(-)-cyclohexanediamine: X-ray structure and CP MAS NMR characterization of [cyclohexylenebis(5-chlorosalicylideneiminato)zinc(II)pyridine] and [cyclohexylenebis(5-bromosalicylideneiminato)zinc(II)pyridine]. *Inorg Chim Acta* **358**, 467–75.
  37. Davis RN, Tanski JM, Adrian JC, Tyler LA (2007) Variations in the coordination environment of  $\text{Co}^{2+}$ ,  $\text{Cu}^{2+}$  and  $\text{Zn}^{2+}$  complexes prepared from a tridentate(imino) pyridine ligand and their structural comparisons. *Inorg Chim Acta* **360**, 3061–8.
  38. Thies S, Näther C, Herges R (2011) 5-Chloro-2-(phenyldiazenyl)pyridine. *Acta Crystallogr* **E67**, o3298.
  39. Kurtoglu M (2010) Synthesis, complexation, spectral, antibacterial and antifungal activity of 2,4-dihydroxy-5-[(E)-phenyldiazenyl] benzaldehyde oxime. *J Serb Chem Soc* **75**, 1231–9.
  40. Prasad KS, Kumar LS, Revanasiddappa HD, ViJay B, Jayalakshmi B (2011) Synthesis, characterization and antimicrobial activity of Cu(II), Co(II), Ni(II), Pd(II) and Ru(III) complexes with clomiphene citrate. *Chem Sci J* **2**, CSJ-28.